TDA Progress Report 42-117

May 15, 1994

A Closed-Loop Time-Alignment System for Baseband Combining

Y. Feria
Communications Systems Research Section

In baseband combining, the key element is the time alignment of the baseband signals. This article describes a closed-loop time-alignment system that estimates and adjusts the relative delay between two baseband signals received from two different antennas for the signals to be coherently combined. This system automatically determines which signal is advanced and delays it accordingly with a resolution of a sample period. The performance of the loop is analyzed, and the analysis is verified through simulation. The variance of the delay estimates and the signal-to-noise ratio degradation in the simulations agree with the theoretical calculations.

I. Introduction

Antenna array combining techniques have been used in the Deep Space Network to improve the signal-to-noise ratio (SNR) [1]. These techniques include full spectrum, baseband, and symbol stream combining. Each technique, however, has been applied only to a specific mission, and a rigorous comparison between the techniques is missing. To have a better understanding of how these techniques perform under the same or different conditions, all techniques are being studied and simulated in software.

This article concentrates on baseband combining where signals from two antennas have each had their carrier removed before going into the combiner. A diagram of baseband (BB) combining is shown in Fig. 1. The signals received from the ith antenna have the following form [1]:

$$\begin{aligned} r_i(t) &= \sqrt{2P_{C_i}}\sin\left(\omega_{c_i}(t-\tau_i)+\theta_{c_i}\right)+\sqrt{2P_{D_i}}d(t-\tau_i) \\ &\quad\times \operatorname{sgn}\left[\sin\left(\omega_{sc}(t-\tau_i)+\theta_{sc}\right)\right] \\ &\quad\times \cos\left(\omega_{c_i}(t-\tau_i)+\theta_{c_i}\right)+n_i(t) \end{aligned} \tag{1}$$

where $P_{C_i} = P_i\cos^2\Delta$ and $P_{D_i} = P_i\sin^2\Delta$, with P_i being the total signal power of the received signal from the ith antenna, and Δ is the modulation index. The parameters ω_{c_i} and θ_{c_i} denote the carrier angular frequency and phase of the received signal from the ith antenna, ω_{sc} and θ_{sc} denote the subcarrier angular frequency and phase, and τ_i is the relative delay between the reference signal and the ith signal. These received signals are analog-to-digital (A/D) converted and downconverted to an intermediate frequency (IF) and then sampled before going through the

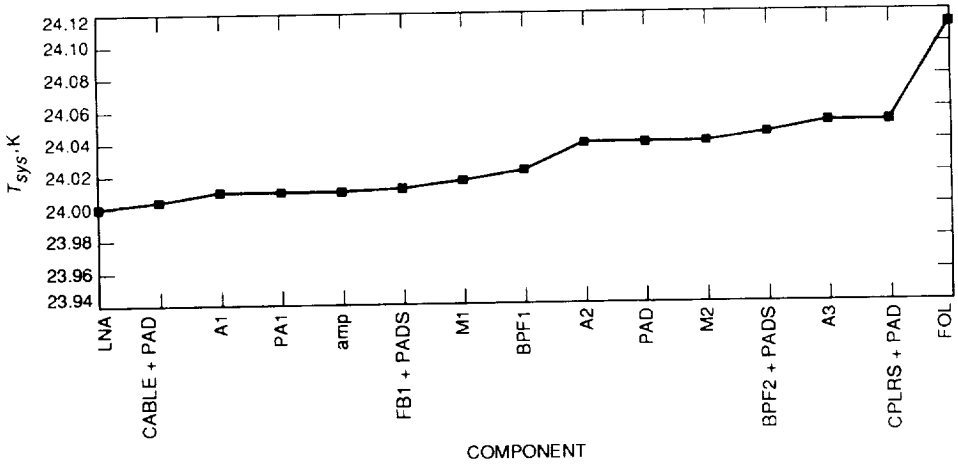

Fig. 6. RF/IF downconverter cumulative system temperature by component.

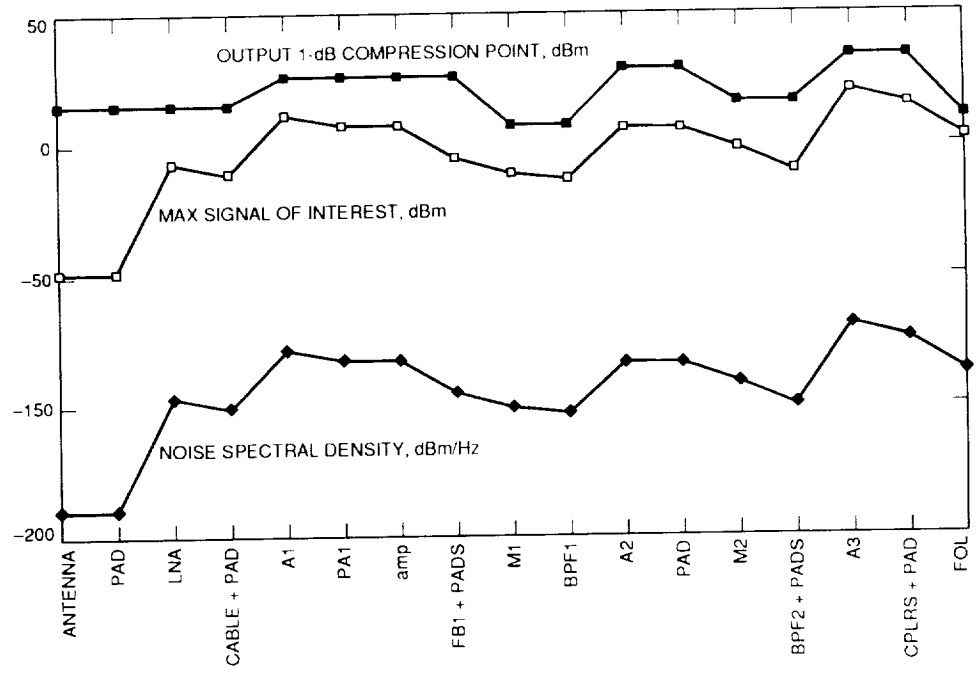

Fig. 7. RF/IF downconverter gain profile.

carrier tracking in the model. After carrier removal, ignoring the filtering effects on the data and the squarewave subcarrier, the signals have the form

$$\begin{aligned} r_i'(k) &= \sqrt{P_{D_i}} \cos \phi_{c_i} d(kT_s - \tau_i) \\ &\quad \times \operatorname{sgn}\left[\sin\left(\omega_{sc}(kT_s - \tau_i) + \theta_{sc}\right)\right] + n_i'(k) \\ &= s_i(k) + n_i'(k) \end{aligned} \tag{2}$$

where T_s denotes the sampling period, and ϕ_{c_i} is the carrier phase error in the ith carrier-tracking loop. The signals $r_i'(k)$, $i = 1, 2, ...,$ are the to-be-combined baseband signals with different time-varying time delays. To coherently combine these signals, it is necessary to align them in time first.

To align two signals in time, first find the relative delay between the two signals. A standard procedure for finding a relative delay between two signals is to correlate them [2] since the cross-correlation is a (linear or nonlinear) function of the relative delay. The advanced signal will then be delayed by the amount computed from the cross-correlation. As mentioned before, the relative delay is not constant in time; therefore, to track the dynamics of the relative delay automatically, a closed loop is used. To close the loop, a number of components need to be added, e.g., a loop filter and an integrator.

This article presents a closed-loop time-alignment system, which takes two baseband signals, estimates the relative delay between the two signals using a correlator, and adjusts the time delay of the advanced signal through a loop filter and an integrator before combining the two baseband signals. The closed-loop time-alignment system, shown in Fig. 2, consists of a quadrature correlator, a loop filter, a unit delay, an integrator, a nearest integer device, and a decision-making device.

Each component in the loop has its function, as briefly described below and in detail in the subsections. The cross-correlator determines the relative delay between two signals. The loop filter tracks the dynamics of the relative delay and maintains the loop stability. The unit delay (z^{-1}) is required to close the loop. The integrator ($z/(z-1)$ transfer characteristic) combines the previously and currently computed relative delays. The nearest integer device is needed because the delay can be adjusted only by an integer number of samples. Finally, the decision-making device decides which signal needs to be delayed.

A similar time-alignment system called the real-time telemetry combiner (RTC) has been developed and analyzed [2,4,5]; however, this closed-loop time-alignment system overcomes the following RTC limitations:

(1) Since the length of the correlator in the RTC is fixed, the correlation feedback is not useful for low SNR and the loop has to be open.

(2) Because cross-correlation uses the product of the sign bits of the two signals, it causes the quantization-noise power to increase from −58.8 to −16.8 dB when compared with 8-bit quantization.

(3) Since the delay can be adjusted only in one branch, the to-be-adjusted branch must be delayed relative to the other branch. However, the signals' advance/delay relationship may change in time as the spacecraft moves and the Earth rotates.

(4) The RTC has an analog feedback to adjust delays, which is not suitable for software or completely digital hardware development.

The closed-loop time-alignment system presented here, on the other hand, has the following features:

(1) An adjustable correlation length to accommodate different SNRs.

(2) Cross-correlation, which is a product of the floating-point samples of the signals, reduces the quantization-noise power by 42 dB with 8-bit quantization.

(3) A decision-making device that automatically delays the advanced signal.

(4) Discrete-delay adjustments suitable for software or completely digital hardware development.

Although this time-alignment system can adjust delays only to the precision of an integer number of samples, accuracy is not a problem when the subcarrier is a perfect square wave and the data transitions are instantaneous. In practice, accuracy is not a problem if the signal is not filtered or the sample rate is much higher than the subcarrier frequency. In the case of a filtered signal sampled at a low rate, an added interpolation on the input waveforms can provide better resolution.

Due to all these differences, the RTC analysis does not apply to the closed-loop time-alignment system proposed

here; therefore, an analysis of the new system is needed. Because of the nonlinear device that takes the nearest integer in the loop, linear system theory, or analysis in the frequency domain or Z-domain, does not apply. The remaining choice is to use time-domain analysis for nonlinear systems even though it is not as straightforward as frequency-domain analysis for linear systems.

A system analysis will be given later, following a more detailed description of each of the components in the closed-loop time-alignment system. Simulation results and comparisons with the theoretical calculations will also be presented.

II. System Description

A block diagram of the closed-loop time-alignment system is shown in Fig. 2, and an equivalent diagram of the closed loop is shown in Fig. 3. In this section, each of the components and their functions are described in detail. The components include a cross-correlator, loop filter, unit delay, integrator, a device that takes the nearest integer, and a device that decides which signal to delay.

A. Cross-Correlator

To find the proportionality between cross-correlator output and relative delay, consider the noise-free case. The cross-correlator, shown in Fig. 4, computes the relative delay by taking the difference between the correlation of Signal 1, $s_1(k)$, with Signal 2 delayed by N_d samples, $s_2(k - N_d)$, and the correlation of Signal 2, $s_2(k)$, with Signal 1 delayed by N_d samples, $s_1(k - N_d)$; the result is divided by two. The correlator output becomes

$$c(m) = \frac{1}{2}\left[s_1(k)s_2(k - N_d) - s_1(k - N_d)s_2(k)\right] \quad (3)$$

where $s_1(k)$ and $s_2(k)$ are defined in Eq. (2).

This cross-correlator is similar to that in RTC [2,4,5], except the cross-correlation is floating point instead of sign bit, and discrete instead of continuous. By using correlations of 8-bit quantized samples, the quantization-noise power reduces from -16.8 dB of the single-bit correlation to -58.8 dB.

The analysis of this cross-correlator is similar to that in [2] except the cross-correlator is discrete instead of continuous. The proportionality of the cross-correlator output and the relative delay is given in Appendix A. Assuming that the signal power is normalized to 1, the correlator output in the linear region ($|m| < N_d$) is

$$\begin{aligned} c(m) &= \left[\frac{4f_{sc} - R_{sym}}{f_s}\right] m \\ &= am \end{aligned} \quad (4)$$

where f_{sc} is the subcarrier frequency, R_{sym} is the symbol rate, and f_s is the sampling rate. Dividing the correlator output by a, one obtains the relative delay m.

Appendix A shows that when the artificial delay, N_d, is one-quarter of the number of samples in a subcarrier period, N_{sc}, the linear region is the longest, which means that larger delays can be tracked. Hence, the correlator is called a quadrature correlator.

In a noisy environment, this output is further averaged over N correlator-output samples to reduce the noise effect.

B. Loop Filter

To close the loop, one needs to add a loop filter for dynamic tracking and loop stability. A higher order loop filter does better dynamic tracking. In this case, however, the relative delay is considered to have low dynamics; hence, only a first-order loop filter is used. That is, the filter transfer function is

$$F(z) = K$$

The choice of K influences the loop stability, loop SNR, and loop bandwidth. These issues will be discussed further in Section III.

C. Integrator, Unit Delay, and Decision Making

The integrator combines past and current delay computations; the unit delay is required to close the loop; and the decision-making device is basically a two-way switch that switches one way when input is positive and switches the other way when input is negative. This decision-making device allows the system to delay whichever signal is advanced.

III. System Analysis

To characterize the system quantitatively, a number of parameters need to be determined. Among them are the filter parameters for loop stability, the loop SNR, the loop bandwidth, and the SNR degradation due to misalignment. Except for loop stability, which depends on the filter parameters only, other parameters such as loop

SNR, loop bandwidth, and SNR degradation depend on the loop-output noise variance. This noise variance is analyzed following a brief analysis of loop stability.

A. Loop Stability

For stability analysis, the noise input in Fig. 3 is ignored because loop stability depends solely on the loop parameters and is input independent. Assume that the relative true delay is an integer multiple of the sample period. This assumption makes the nonlinear nearest integer device negligible in a noise-free environment. Note that when the delay is not an integer multiple of a sample period, the nearest integer device can be modeled as an additive quantization noise source of finite magnitude and thus can be ignored for the stability analysis.

Consider a first-order loop filter, $F(z) = K$. The open-loop transfer function is

$$G(z) = Kz^{-2}\frac{z}{z-1}$$

and the closed-loop transfer function is

$$\begin{aligned} H(z) &= \frac{G(z)}{1+G(z)} \\ &= \frac{K}{z^2 - z + K} \end{aligned} \tag{5}$$

A root-locus plot of this system with a first-order loop filter is shown in Fig. 5. From this plot, it can be observed that when $K \geq 1$, the root locus is outside the unit circle; thus, the loop is unstable. For $0.25 < K < 1$, the system is underdamped; for $K = 0.25$, it is critically damped; and for $0 < K < 0.25$, it is overdamped. Besides affecting system stability, the choice of K also affects the noise performance in the delay estimates, as will be discussed.

B. Noise Analysis

To analyze the noise, we first determine the amount of noise (mean and variance) at the output of the quadrature correlator in Fig. 4. This amount of noise is added at the output of the correlator, which acts as a unit delay in the closed loop, as shown in Fig. 6. The noise statistics at the correlator output are given next, followed by the noise statistics of the closed loop. Because of the nonlinear device of taking the nearest integer, the Z-domain linear system theory cannot be applied here, and time-domain analysis is used instead.

1. Noise Variance at Correlator Output. To determine the noise variance at the output of the correlator shown in Fig. 4, assume that the samples of the two inputs to the correlator consist of the sum of baseband signals, $s_1(k)$ and $s_2(k)$ as defined in Eq. (2), and independent samples of additive white Gaussian noise, $n_1'(k)$ and $n_2'(k)$, both with zero mean and variance σ_{in}^2. Denote the kth sample of the inputs of the quadrature correlator as

$$r_i'(k) = s_i(k) + n_i'(k) \tag{6}$$

where $i = 1, 2$.

The output of the correlator before "sum and dump" is

$$q(k) = \frac{1}{2}[r_1'(k)r_2'(k - N_d) - r_1'(k - N_d)r_2'(k)] \tag{7}$$

The sum-and-dump filter takes the average of its input over N samples, and its ouput is then divided by the slope a to produce an output sample

$$w_m = \frac{1}{aN}\sum_{k=mN+1}^{(m+1)N} q(k) \tag{8}$$

where a is defined in Eq. (4).

The problem here is to find the variance of w_m. With the assumption that $\{w_m\}$ is a stationary sequence and the noise samples at the inputs of the correlator are independent and identically distributed with zero mean, the variance of w_m is found to be

$$\sigma_w^2 = \frac{1}{(2a)^2 N}[2\sigma_{in_1}^2\sigma_{in_2}^2 + 4\sigma_{in_1}^2 P_2 + 4\sigma_{in_2}^2 P_1] \tag{9}$$

which is independent of m, and where $P_i, i = 1, 2$ is the ith signal power, and $\sigma_{in_i}^2$ is the ith noise variance at each correlator input. See Appendix B.

2. Noise Variance at Loop Output. An equivalent diagram of the closed loop is shown in Fig. 6, where noise is the input and the output corresponds to the location of the computed delay. Denote the kth noise samples at the input of the loop as w_k, those at the output of the integrator as x_k, and those after taking the nearest integer as y_k. The goal here is to find the variance at the output after the nearest integer device, that is, the variance of y.

The difference equation that describes the closed loop in Fig. 6 is

$$x_k - x_{k-1} = K(w_{k-1} - y_{k-2}) \tag{10}$$

Assuming that w and x are stationary Gaussian random processes with zero mean, then y also has zero mean, and the variances of w, x, and y, denoted by σ_w^2, σ_x^2, and σ_y^2, are found to have the following relationship (Appendix C):

$$\frac{2K}{1+K}\sigma_x^2 - K^2\sigma_y^2 = K^2\sigma_w^2 \tag{11}$$

The relationship between the variances of x and y is

$$\sigma_y^2 = \sum_k p_k k^2 \tag{12}$$

where

$$p_k = \int_{k-\frac{1}{2}}^{k+\frac{1}{2}} \frac{1}{\sqrt{2\pi\sigma_x^2}} e^{-x^2/(2\sigma_x^2)} dx \tag{13}$$

One can solve Eqs. (11), (12), and (13), for σ_y^2 for a given input noise variance σ_w^2. Note that in the absence of the nearest integer device, $\sigma_y^2 = \sigma_x^2$, and Eq. (11) becomes

$$\frac{2 - K^2 - K}{K^2 + K}\sigma_y^2 = \sigma_w^2 \tag{14}$$

which is exactly the same as Eq. (D-3) in Appendix D, in the linear system case.

Also note that for a large input noise variance ($\sigma_w^2 > 0.5$, observed from simulations), the noise generated by the nonlinear nearest integer device is approximated by a quantization noise with a uniform distribution and a variance of one-twelfth, or

$$\sigma_y^2 = \sigma_x^2 + \frac{1}{12}$$

C. Loop SNR and Loop Bandwidth

The loop SNR is usually defined as [1]

$$\rho = \frac{1}{\sigma_\tau^2} \tag{15}$$

where σ_τ^2 is the linear loop-output noise variance in units of squared radians.

However, the loop-output noise variance, σ_y^2, has units of squared number of samples. Converting the units to squared radians by equating a symbol duration to a cycle or 2π radians, one has

$$\sigma_\tau^2 = \left(\frac{2\pi R_{sym}}{f_s}\right)^2 \sigma_y^2 \tag{16}$$

where f_s is the sampling rate, and R_{sym} is the data rate. The loop SNR can be expressed as

$$\rho = \left(\frac{f_s}{2\pi R_{sym}}\right)^2 \frac{1}{\sigma_y^2} \tag{17}$$

The one-sided noise equivalent bandwidth for a linear system is defined as [4]

$$B_L = \frac{1}{2T_L} I_2 \tag{18}$$

where

$$I_2 = \frac{1}{|H(z)|^2} \frac{1}{2\pi j} \oint_{|z|=1} H(z)H(z^{-1}) \frac{1}{z} dz$$

$H(z)$ is the closed-loop transfer function, $T_L = NT_s$ is the correlation time, N is the number of samples in the correlation, and T_s is the original sample period. The loop input and output variances are related through I_2, that is, $var_{out} = I_2 var_{in}$. Note that var_{in} and var_{out} are not the same as σ_{in}^2 and σ_{out}^2 used previously.

In a nonlinear system, however, Z-domain analysis is no longer valid; thus, there is not an expression for $H(z)$, nor for I_2. Therefore, the loop bandwidth cannot be defined the same way as for linear systems. However, an expression for the relation between the input and output variances is available in Eq. (11); hence, the one-sided noise equivalent bandwidth is defined in this case as

$$B_L \equiv \frac{1}{2T_L} \frac{var_{out}}{var_{in}}$$

$$= \frac{1}{2T_L} \frac{\sigma_y^2}{\sigma_w^2} \tag{19}$$

where σ_y^2 and σ_w^2 have been defined in Sections III.B.1 and III.B.2.

D. SNR Degradation Due to the Loop

The magnitude reduction of the signal at the output of the sum-and-dump filter due to time misalignment in the baseband-combining scheme is (see Appendix E)

$$C_{\tau_i} = 1 + \left(\frac{1}{2} - 2\frac{f_{sc}}{R_{sym}}\right)\tau_i \tag{20}$$

where τ_i is the relative delay over a symbol period between the ith antenna and the reference antenna. Note that the expression in Eq. (20), derived in Appendix E, differs from the stated expression in Eq. 39 in [1] for the baseband-combining assembly containing the RTC. The first and second moments of the reduction function of the time-alignment loop are

$$\overline{C}_{\tau_i} = 1 + \left(\frac{1}{2} - 2\frac{f_{sc}}{R_{sym}}\right)\sqrt{\frac{2}{\pi}}\sigma_{\tau_i} \tag{21}$$

and

$$\overline{C_{\tau_i}^2} = 1 + 2\left(\frac{1}{2} - 2\frac{f_{sc}}{R_{sym}}\right)\sqrt{\frac{2}{\pi}}\sigma_{\tau_i} + \left(\frac{1}{2} - 2\frac{f_{sc}}{R_{sym}}\right)^2\sigma_{\tau_i}^2 \tag{22}$$

where $i = 1, 2$. Note that $\overline{C_{\tau_1}} \equiv 1$, and $\overline{C_{\tau_1}^2} \equiv 1$, which implies $\sigma_\tau = 0$.

Assuming perfect carrier and subcarrier tracking and symbol synchronization, the degradation due solely to the closed-loop time-alignment system is

$$D_{ta} = 10\log_{10}\left[\frac{\sum_{i=1}^{N_a}\gamma_i^2\overline{C_{\tau_i}^2} + \sum_{i,j,i\neq j}\gamma_i\gamma_j\overline{C}_{\tau_i}\overline{C}_{\tau_j}}{\Gamma^2}\right] \tag{23}$$

where $\gamma_i = (P_i/N_{o_i})/(P_1/N_{o_1})$, and $\Gamma = \sum_{i=1}^{N_a}\gamma_i$, with N_a being the number of antennas in the array, which is 2 in this case.

Having analyzed and defined all the necessary parameters, we now can check theoretical versus simulation results.

IV. Simulation Results

To verify the theoretical results, the P_t/N_o at the input of the cross correlator is fixed at 45 dB-Hz. The loop gain K is set at 0.25, and the sample rate at 500 kHz. The subcarrier frequency is 5 kHz, and the symbol rate is 1000 symbols/sec. There is no carrier in the simulation since the carrier is tracked and removed before baseband combining. The cross-correlation length N (or loop bandwidth B_L) is varied, and the loop SNR, ρ, is obtained from the theory and the simulations. The results are shown in Table 1 and the comparison of the results is shown in Fig. 7.

The simulation results also show that when the noise standard deviation at the input of the closed loop, σ_w, is larger than the one-sided length of the linear region, N_d, ($\sigma_w > N_d$) the loop fails to track. This can be observed in Fig. 7 for ρ smaller than 17 dB.

The SNR degradation due to the closed-loop time-alignment system is also measured through simulation and the results are very close to those obtained from Eq. (23), as shown in Table 2. The parameters in the simulations are as follows: Assume two identical antennas, each with $P_t/N_o = 23.54$ dB-Hz. The modulation index is 70 deg. The sampling rate is 100,000 Hz; the carrier frequency is 3 Hz; the subcarrier frequency is 1000 Hz; and the symbol rate is 200 symbols/sec. The time-alignment loop gain, K, is 0.0625. Simulations are done for two cases, with a perfect time alignment and with the closed-loop time-alignment system. The difference in SNR degradation is due to the closed-loop time-alignment system.

V. Conclusions

The article gives a full description of the design of a closed-loop time-alignment system and a detailed description of each of the elements in the system. It also provides an analysis of loop stability, noise effect, loop bandwidth, loop SNR in terms of the length of the correlation, and SNR degradation due to the loop. The closed-loop time-alignment system described here differs from the RTC in that this system is fully digital and is suitable for software and completely digital hardware implementation. The correlation is performed with floating-point samples of the to-be-combined signals rather than their sign bits. This causes the quantization-noise power to drop from -16.8 to

−58.8 dB in the correlation, assuming 8-bit quantization. The delay can be adjusted in either branch rather than a single branch only. The length of the cross-correlation can be adjusted for different levels of SNR. Because delays are adjusted digitally, an operation to take the nearest integer is needed, which results in a nonlinear system. An analysis of the nonlinear system is presented in the article. The noise analysis of this loop is significantly different from that of the RTC, due to the floating-point cross-correlation and the nonlinearity. The article also gives a well-matched comparison of theoretical and simulated results. The linear region of the relationship between the cross-correlation and the delay is determined. When the standard deviation of the delay estimates exceeds a quarter of the subcarrier period, the relationship between the cross-correlation and the delay is no longer linear, which corresponds to about a 17-dB loop SNR.

Although the time-alignment system described in this article aligns two signals, it can be easily expanded into the alignment of N_a signals, where $N_a > 2$, by aligning the signals pairwise in N layers, where $N = \lceil \log_2 N_a \rceil$. It can be shown that the total number of alignments is $N_a - 1$, which is the same as if we chose the signal with the longest delay as the reference, and adjusted all the delays of the $N_a - 1$ signals one by one as in [1]. Two advantages of aligning the signals pairwise using this scheme are

(1) No reference signal is needed as this reference may need to be changed in time.

(2) The SNRs get stronger after each layer, thus enabling the computation time to be reduced.

The combining degradation still needs to be analyzed.

Some simulation results show that this time-alignment system can be improved by low-pass filtering the to-be-correlated signals before the quadrature correlator. However, further analysis is needed to completely characterize the system and the associated improvement.

Acknowledgments

The author would like to thank Dr. Sam Dolinar, Dr. Sami Hinedi, Larry Howard, Alexander Mileant, Biren Shah, Dr. Marv Simon, and Dr. Steve Townes for their many helpful suggestions and discussions. The author is also very thankful to Samson Million for his assistance in implementing the system.

References

[1] A. Mileant and S. Hinedi, "Overview of Arraying Techniques in the Deep Space Network," *The Telecommunications and Data Acquisition Progress Report 42-104, vol. October–December 1990*, Jet Propulsion Laboratory, Pasadena, California, pp. 109–139, February 15, 1991.

[2] R. A. Winkelstein, "Analysis of the Signal Combiner for Multiple Antenna Arraying," *JPL Deep Space Network Progress Report 42-26, vol. January–February 1975*, Jet Propulsion Laboratory, Pasadena, California, pp. 102–118, April 15, 1975.

[3] E. I. Jury, *Theory and Application of the Z-Transform Method*, Malabar, Florida: Robert E. Krieger Publishing Co., 1964.

[4] M. K. Simon and A. Mileant, *Performance of the DSN Baseband Assembly (BBA) Real-Time Combiner (RTC)*, JPL Publication 84-94, Revision 1, Jet Propulsion Laboratory, Pasadena, California, May 1, 1985.

[5] L. D. Howard, "Prototype Real-Time Baseband Signal Combiner," *The Telecommunications and Data Acquisition Progress Report 42-60, vol. September–October 1980*, Jet Propulsion Laboratory, Pasadena, California, pp. 145–151, December 15, 1980.

Table 1. Performance of the time-alignment closed loop.

N	B_L, Hz	$\sigma_w^2(theo)$	$\sigma_y^2(theo)$	ρ_{theo}, dB	ρ_{simu}, dB	$\rho_{simu} - \rho_{theo}$, dB
25	1821.6	1303.6	237.47	14.26	3.17	−11.08
40	1157.1	814.8	150.85	16.23	9.82	−6.41
50	926.6	651.8	120.79	17.20	17.13	−0.07
100	463.7	325.9	60.45	20.20	20.13	−0.07
200	232.2	163.0	30.28	23.20	23.32	0.11
400	116.5	81.5	15.19	26.20	26.40	0.20
800	58.7	40.7	7.64	29.18	29.13	−0.05
1600	29.6	20.4	3.87	32.14	32.32	0.18

Table 2. SNR degradation due to the time-alignment closed loop.

N	B_L, Hz	ρ, dB	$\sigma_y^2(theo)$	$\sigma_y^2(simu)$	D_{theo}, dB	D_{simu}, dB
10,000	0.172	19.21	75.97	83.11	−0.92	−1.11
50,000	0.035	26.18	15.26	15.48	−0.39	−0.38
500,000	0.0036	35.96	1.60	2.45	−0.14	−0.13
5,000,000	4.58×10^{-4}	44.96	0.20	0.00	0.00	0.00

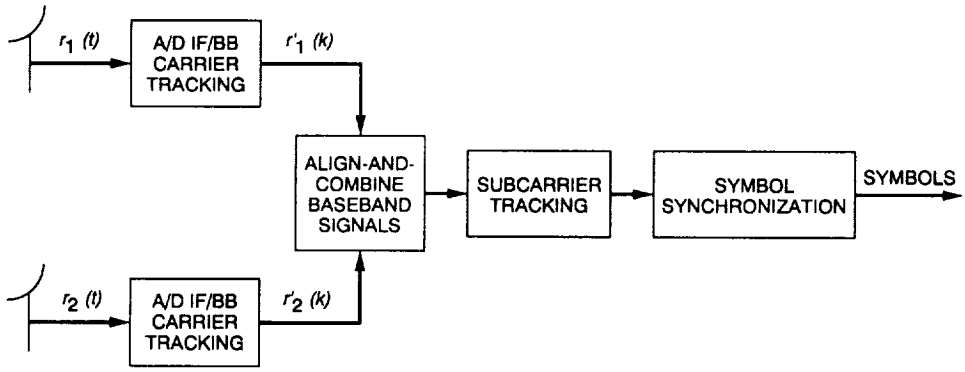

Fig. 1. A diagram of baseband combining of two signals.

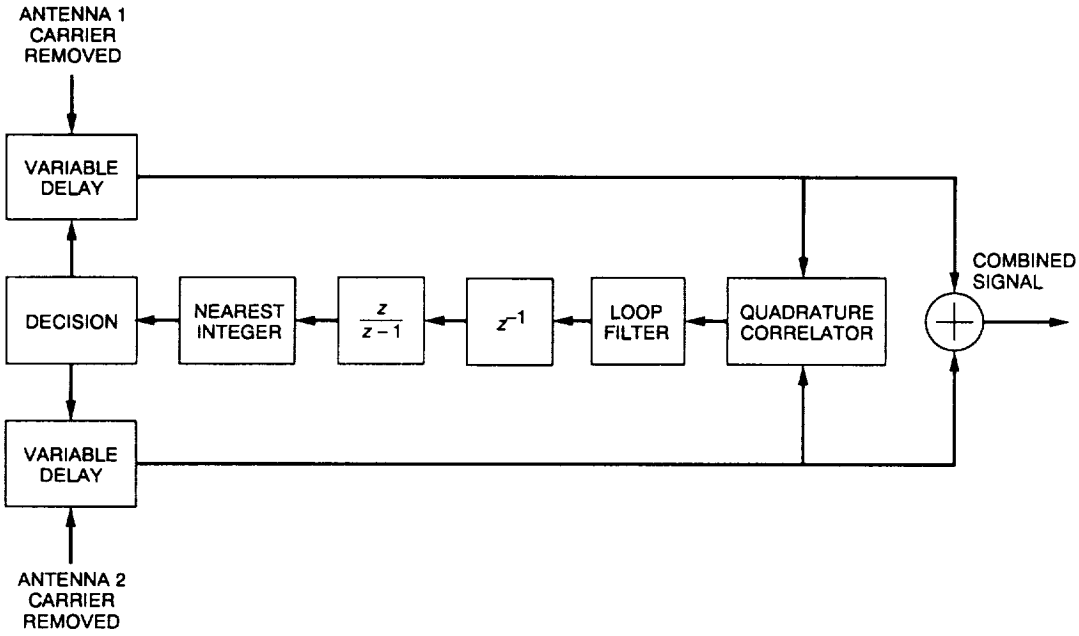

Fig. 2. A closed-loop time-alignment system.

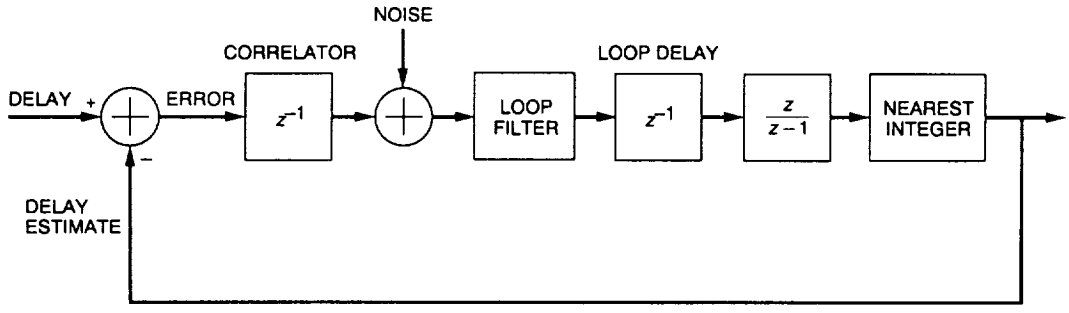

Fig. 3. An equivalent diagram of the closed-loop time-alignment system.

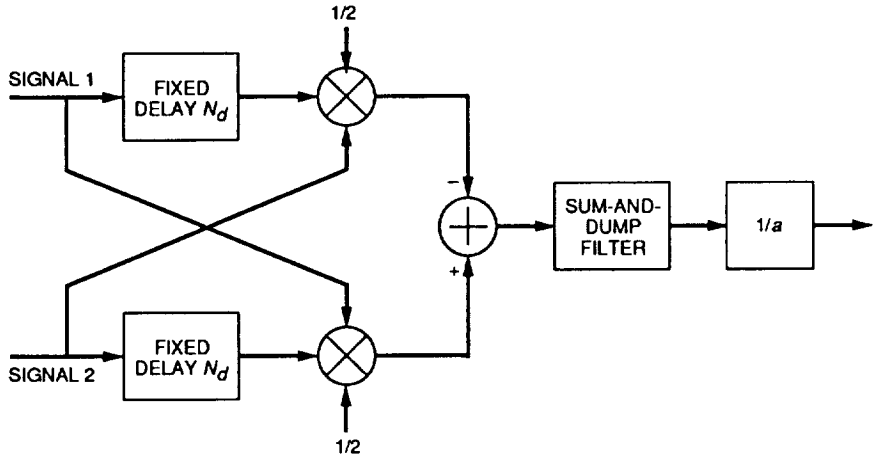

Fig. 4. A diagram of the quadrature correlator.

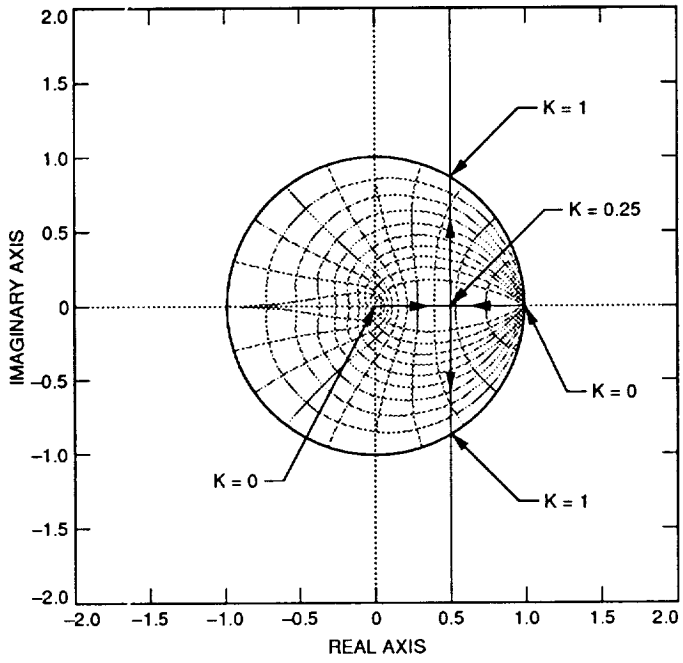

Fig. 5. Root locus for the first-order loop filter.

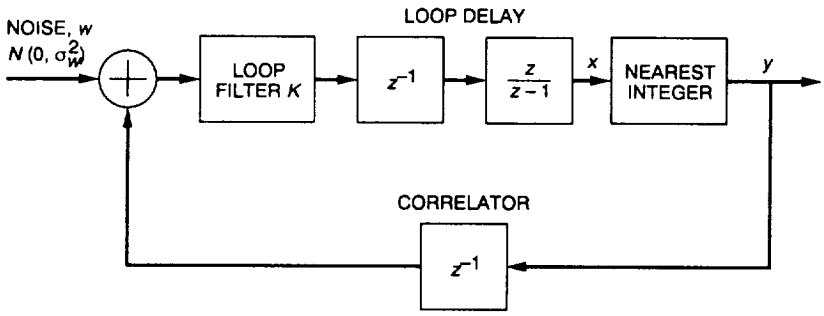

Fig. 6. The equivalent noise diagram.

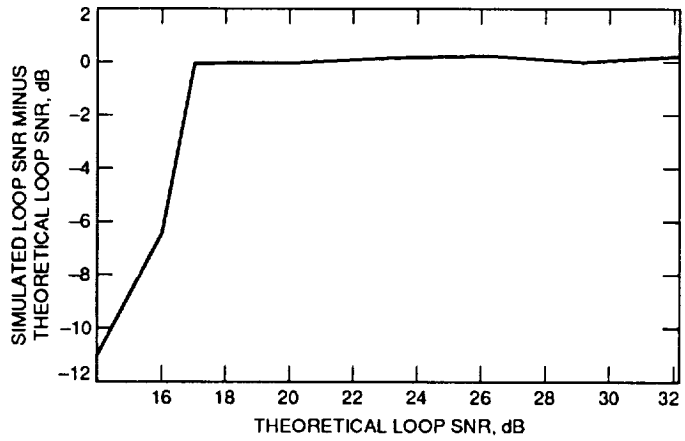

Fig. 7. Comparison of theoretical and simulated loop SNR.

Appendix A

Correlator Output Versus Relative Delay

The following gives the proportionality between the cross-correlator output and the relative delay between the signals received from two antennas. Let N_{sc} be the number of samples in a subcarrier period, N_{sy} the number of samples in a symbol period, and N_d the number of samples in the artificial delay. As stated before, a baseband signal consists of data on a square-wave subcarrier. Assuming that the data and the subcarrier are independent, the autocorrelation of the product of the data times the subcarrier equals the product of the autocorrelation of the data and that of the subcarrier. Considering the linear region $|m| < N_{sc}/2$, the data correlation function is

$$c_{data}(m) = 1 - \frac{|m|}{N_{sy}} \tag{A-1}$$

and the subcarrier correlation function is

$$c_{sc}(m) = 1 - \frac{|m|}{N_{sc}/4} \tag{A-2}$$

The correlation of data times subcarrier is

$$c_{(data)(sc)}(m) = 1 - \frac{|m|}{N_{sc}/4} - \frac{|m|}{N_{sy}} + \frac{m^2}{N_{sy}N_{sc}/4} \tag{A-3}$$

Then correlation curves are delayed or advanced by N_d samples, which is equivalent to the correlations of $s_1(k - N_d)s_2(k)$ or $s_1(k)s_2(k - N_d)$. That is, in the region of $[-N_{sc}/2 + N_d, N_d]$, the correlation function is

$$c_{(s_{1_{delayed}})} = 1 + \frac{m - N_d}{N_{sc}/4} + \frac{m - N_d}{N_{sy}} + \frac{(m - N_d)^2}{N_{sy}N_{sc}/4} \tag{A-4}$$

and in the region of $[-N_d, N_{sc}/2 - N_d]$

$$c_{(s_{2_{delayed}})} = 1 - \frac{m + N_d}{N_{sc}/4} - \frac{m + N_d}{N_{sy}} + \frac{(m + N_d)^2}{N_{sy}N_{sc}/4} \tag{A-5}$$

Finally, taking the difference of these two correlations and dividing the result by 2, one obtains an equation of the cross-correlator output in the linear region:

$$c(m) = \frac{4f_{sc} - R_{sym}}{f_s} m = am \tag{A-6}$$

where f_s is the sampling frequency, f_{sc} is the subcarrier frequency, and R_{sym} is the symbol rate.

It is clear that the longer the linear region, the larger the relative delay that can be tracked. The linear region is longest when the regions $[-N_{sc}/2 + N_d, N_d]$ and $[-N_d, N_{sc}/2 - N_d]$ coincide. That is, when

$$N_d = N_{sc}/4$$

Hence, the cross-correlator is also called a quadrature correlator.

Figure A-1 shows a special case where the number of samples per symbol period is chosen to be $N_{sy} = 10$, the number of samples per subcarrier period is $N_{sc} = 8$, and the number of samples in the delay is $N_d = N_{sc}/4 = 2$ to demonstrate the correlation of random data, a square-wave subcarrier, and their product. Note that N_{sy} and N_{sc} are arbitrarily chosen with a condition that $N_{sy} > N_{sc}$.

The first part of Fig. A-2 shows the correlation of $s_1(k - N_d)$ and $s_2(k) = s_1(k-m)$, which is the correlation of $s_1(k)$ and $s_2(k)$ shifted to the right by N_d samples. Similarly, the correlation of $s_1(k)$ and $s_2(k - N_d) = s_1(k - N_d - m)$ is the correlation of $s_1(k)$ and $s_2(k)$ shifted to the left by N_d samples. The second part of Fig. A-2 takes the difference between these two correlations and divides the result by 2, so that a linear region can be observed from $-N_d$ to N_d, with N_d being 2 in this case. Figure A-3 confirms that the maximum length of the linear region occurs when $N_d T_s$ is chosen to be one-quarter of the subcarrier period.

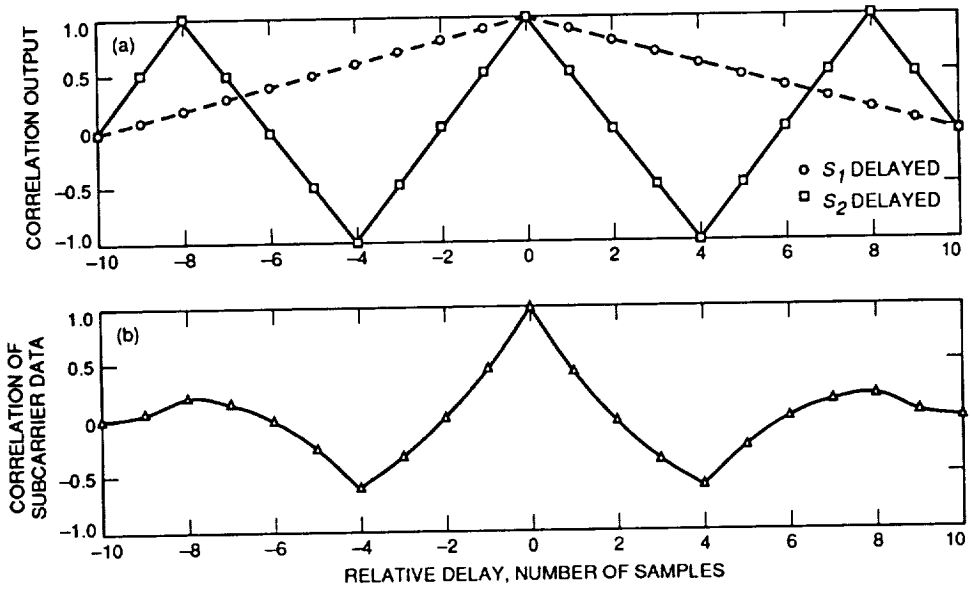

Fig. A-1. Autocorrelations of (a) PN to the square-wave subcarrier, and (b) to their products, $N_{SC} = 8$ and $N_{SY} = 10$.

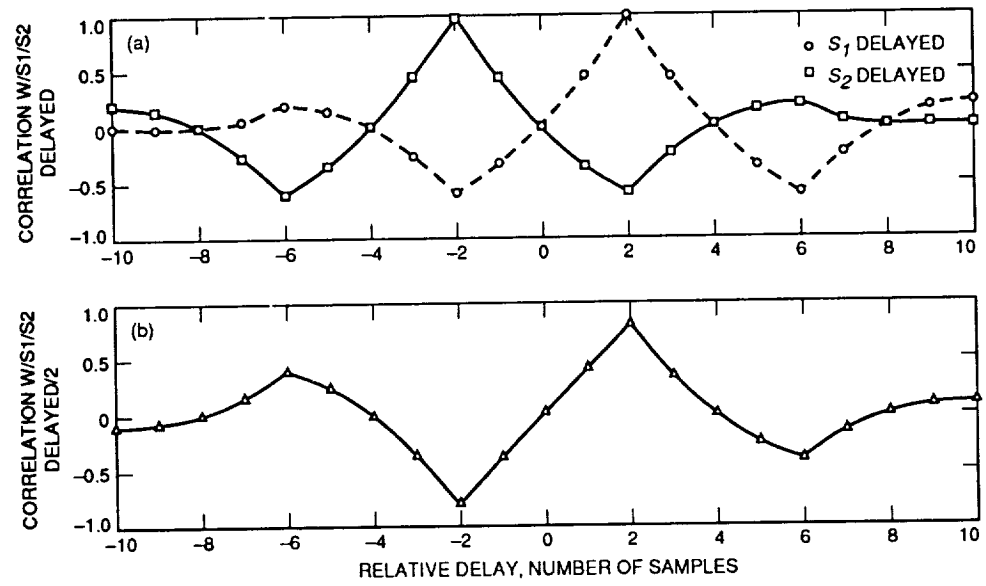

Fig. A-2. The correlation (a) signals S_1 and S_2 delayed and (b) their difference over 2.

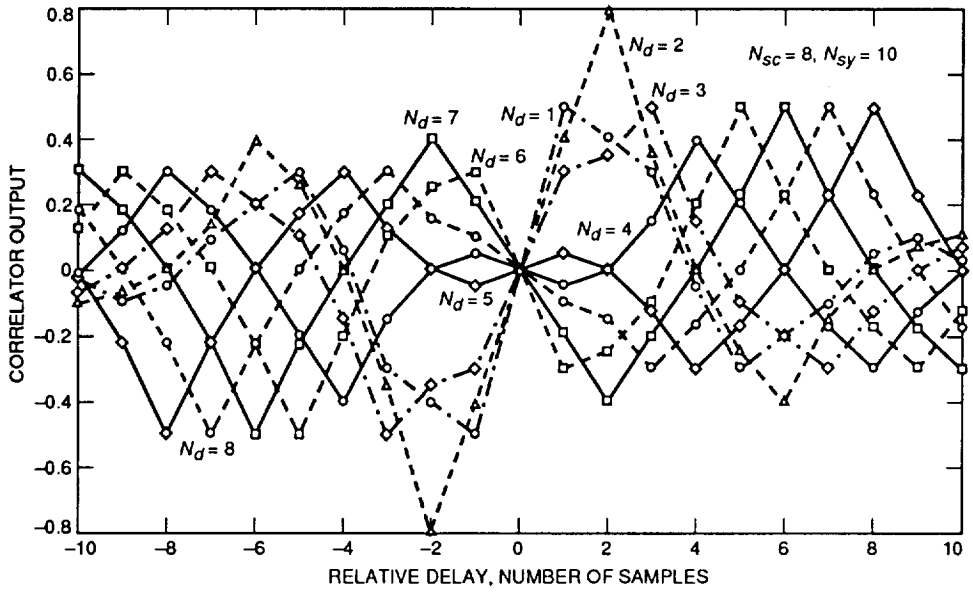

Fig. A-3. Linear-region length in the "S-curve" depends on N_d.

Appendix B

Noise Variance at the Correlator Output

To find the noise variance at the correlator output, we initially find the first and second moments of the correlation. Assuming that the correlation $\{w_m\}$ is stationary (and noting that the index m can be dropped), then its first moment is

$$\begin{aligned} E\{w\} &= \frac{1}{aN}\sum_{k=1}^{N} E\{q(k)\} \\ &= \frac{1}{2aN}\sum_{k=1}^{N} E\{r_1'(k)r_2'(k-N_d) - r_1'(k-N_d)r_2'(k)\} \\ &= \frac{1}{2aN}\sum_{k=1}^{N} E\{s_1(k)s_2(k-N_d) \\ &\quad - s_1(k-N_d)s_2(k)\} \end{aligned} \tag{B-1}$$

The square of the first moment is

$$\begin{aligned} (E\{w\})^2 &= \frac{1}{(2aN)^2}\sum_{k=1}^{N}\sum_{m=1}^{N} E\{s_1(k)s_2(k-N_d) \\ &\quad - s_1(k-N_d)s_2(k)\} \\ &\quad \times E\{s_1(m)s_2(m-N_d) \\ &\quad - s_1(m-N_d)s_2(m)\} \\ &\quad + E\{s_1(k)s_1(m)s_2(k-N_d)s_2(m-N_d)\} \\ &\quad - E\{s_1(k)s_1(m-N_d)s_2(k-N_d)s_2(m)\} \\ &\quad - E\{s_1(k-N_d)s_1(m)s_2(k)s_2(m-N_d)\} \\ &\quad + E\{s_1(k-N_d)s_1(m-N_d)s_2(k) \\ &\quad \times s_2(m)\} \end{aligned} \tag{B-2}$$

The second moment of w is defined as

$$E\{w^2\} = \frac{1}{(2aN)^2}\sum_{k=1}^{N}\sum_{m=1}^{N} E\{q(k)q(m)\} \tag{B-3}$$

Denote the variances of the noises at the correlator inputs as $\sigma_{in_1}^2$ and $\sigma_{in_2}^2$ and the signal powers as P_1 and P_2, respectively. Expanding the product $q(k)q(m)$, one obtains

$$\begin{aligned} E\{w^2\} &= \frac{1}{(2aN)^2}\sum_{k=1}^{N}\sum_{m=1}^{N} [2\sigma_{in_1}^2\sigma_{in_2}^2\delta_{m,k} \\ &\quad + 2\sigma_{in_2}^2 P_1\delta_{m,k} + 2\sigma_{in_1}^2 P_2\delta_{m,k} \\ &\quad - \sigma_{in_2}^2 E\{s_1(k)s_1(k-2N_d)\}\delta_{m,k-N_d} \\ &\quad - \sigma_{in_2}^2 E\{s_1(k+N_d)s_1(k-N_d)\}\delta_{m,k+N_d} \\ &\quad - \sigma_{in_1}^2 E\{s_2(k)s_2(k-2N_d)\}\delta_{m,k-N_d} \\ &\quad - \sigma_{in_1}^2 E\{s_2(k+N_d)s_2(k-N_d)\}\delta_{m,k+N_d} \\ &\quad + E\{s_1(k)s_1(m)s_2(k-N_d)s_2(m-N_d)\} \\ &\quad - E\{s_1(k)s_1(m-N_d)s_2(k-N_d)s_2(m)\} \\ &\quad - E\{s_1(k-N_d)s_1(m)s_2(k)s_2(m-N_d)\} \\ &\quad + E\{s_1(k-N_d)s_1(m-N_d) \\ &\quad \times s_2(k)s_2(m)\}] \end{aligned} \tag{B-4}$$

For a quadrature correlator, the delay N_d is one-quarter of the subcarrier period; thus, two points of the same signal that are $2N_d$ samples apart are one-half of a period apart, which means that they always have the same magnitude and the opposite sign. Therefore, their product is $-P_i$, $i = 1, 2$. Also note that the last four terms in Eq. (B-4) are the mean squared of w, which is subtracted from $E\{w^2\}$ to obtain the variance of w; hence, the variance of w is

$$\sigma_w^2 = \frac{1}{(2a)^2 N}[2\sigma_{in_1}^2\sigma_{in_2}^2 + 4\sigma_{in_2}^2 P_1 + 4\sigma_{in_1}^2 P_2] \tag{B-5}$$

Appendix C

Noise Variance at the Loop Output

The difference equation that describes the closed loop in Fig. 6 is

$$x_k - x_{k-1} = K(w_{k-1} - y_{k-2}) \tag{C-1}$$

Assuming that w and x are stationary zero-mean Gaussian processes, taking the expected value of Eq. (C-1), one obtains

$$E\{y\} = 0$$

Then the second moments of the processes w, x, and y are their variances denoted by σ_w^2, σ_x^2, and σ_y^2, respectively. Now taking the expected value on both sides of Eq. (C-1) squared,

$$E\{x_k^2\} - 2E\{x_k x_{k-1}\} + E\{x_{k-1}^2\} =$$

$$K^2(E\{w_{k-1}^2\} + E\{y_{k-2}^2\}) \tag{C-2}$$

That is

$$2\sigma_x^2 = K^2\sigma_w^2 + K^2\sigma_y^2 + 2E\{x_k x_{k-1}\} \tag{C-3}$$

The last term in Eq. (C-3) can be expressed in terms of the variance of x when multiplying Eq. (C-1) by x_{k-1} and taking the expected value. That is,

$$E\{x_k x_{k-1}\} = E\{x_{k-1}^2\} + KE\{w_{k-1}x_{k-1}\}$$

$$- KE\{x_{k-1}y_{k-2}\} \tag{C-4}$$

To see that $E\{w_{k-1}x_{k-1}\} = 0$, one can multiply Eq. (C-1) by w_k:

$$E\{w_n x_n\} = E\{w_n x_{n-1}\} + KE\{w_n w_{n-1}\}$$

$$- KE\{w_n y_{n-2}\} = 0 \tag{C-5}$$

The last step in the above equation follows since the past outputs are independent of the future inputs when the system is causal and the noises at different times are independent. Going back to Eq. (C-4), since y_{k-2} is the nearest integer of x_{k-2}, it can be expressed through an ϵ_{k-2} as

$$y_{k-2} = x_{k-2} + \epsilon_{k-2}$$

where ϵ_{k-2} represents a quantization error. Substituting the above into Eq. (C-4), one has

$$E\{x_k x_{k-1}\} = \sigma_x^2 - KE\{x_{k-1}x_{k-2}\}$$

$$- KE\{x_{k-1}\epsilon_{k-2}\} \tag{C-6}$$

The last term in Eq. (C-6) is zero since the past output ϵ_{k-2} is independent of the future input x_{k-1}. Applying the stationary property of x and rearranging Eq. (C-6), one obtains

$$E\{x_k x_{k-1}\} = \frac{1}{1+K}\sigma_x^2 \tag{C-7}$$

Substituting Eq. (C-7) into Eq. (C-3), one has

$$\frac{2K}{1+K}\sigma_x^2 - K^2\sigma_y^2 = K^2\sigma_w^2 \tag{C-8}$$

Appendix D

Noise Variance at Loop Output for Linear Cases

Without taking the nearest integer, the linear system theory should be applied. The variance at the output of the loop y equals the variance of the delay estimates due to the noise n, and it is

$$\sigma_y^2 = \frac{1}{|H(1)|^2}\sigma_w^2 I_2$$

where

$$I_2 = \frac{1}{2\pi j}\oint_{|z|=1} H(z)H(z^{-1})\frac{1}{z}dz$$

Using the first-order loop filter, the closed-loop transfer function is

$$H(z) = \frac{Kz}{z^2 - z - K} \tag{D-1}$$

Using the formula given in [3], I_2 is

$$I_2 = \frac{K^2 + K}{2 - K - K^2} \tag{D-2}$$

The variance of y is

$$\sigma_y^2 = \frac{K^2 + K}{2 - K - K^2}\sigma_w^2 \tag{D-3}$$

Appendix E

Signal Amplitude Reduction Due to Misalignment

Let N_{sc}, N_{sy}, and N_{rd} be the number of samples per subcarrier period, symbol duration, and in the relative delay. First, consider the ideal case where the signals are perfectly aligned, and the combined signal amplitude at the output of the sum-and-dump filter is

$$A_{ideal} = 2N_{sy}$$

Then consider adding two misaligned signals. The signal amplitude at the output of the sum-and-dump filter becomes

$$A_{mis} = \frac{1}{2}\left[2\left(\frac{N_{sc}}{2} - N_{rd}\right)\right] + \frac{1}{2}2\frac{N_{sc}}{2} + \left(2\frac{N_{sy}}{N_{sc}} - 1\right)2\left(\frac{N_{sc}}{2} - N_{rd}\right) \quad \text{(E-1)}$$

The amplitude reduction of the misaligned signal at the output of the sum-and-dump filter is

$$\begin{aligned} C_i &= \frac{A_{mis}}{A_{ideal}} \\ &= 1 - 2\frac{N_{sy}}{N_{sc}}\frac{N_{rd}}{N_{sy}} + \frac{1}{2}\frac{N_{rd}}{N_{sy}} \\ &= 1 + \left(\frac{1}{2} - 2\frac{N_{sy}}{N_{sc}}\right)\tau_i \\ &= 1 + \left(\frac{1}{2} - 2\frac{f_{sc}}{R_{sym}}\right)\tau_i \end{aligned} \quad \text{(E-2)}$$

where f_{sc} is the subcarrier frequency, R_{sym} is the symbol rate, and

$$\tau_i = \frac{N_{rd}}{N_{sy}}$$

is the relative delay between the ith signal and the reference signal in terms of a symbol period.

N94-35553

TDA Progress Report 42-117

May 15, 1994

Correlator Data Analysis for the Array Feed Compensation System

B. Iijima and D. Fort
Tracking Systems and Applications Section

V. Vilnrotter
Communications Systems Research Section

The real-time array feed compensation system is currently being evaluated at DSS 13. This system recovers signal-to-noise ratio (SNR) loss due to mechanical antenna deformations by using an array of seven Ka-band (33.7-GHz) horns to collect the defocused signal fields. The received signals are downconverted and digitized, in-phase and quadrature samples are generated, and combining weights are applied before the samples are recombined. It is shown that when optimum combining weights are employed, the SNR of the combined signal approaches the sum of the channel SNRs. The optimum combining weights are estimated directly from the signals in each channel by the Real-Time Block II (RTB2) correlator; since it was designed for very-long-baseline interferometer (VLBI) applications, it can process broadband signals as well as tones to extract the required weight estimates. The estimation algorithms for the optimum combining weights are described for tones and broadband sources. Data recorded in correlator output files can also be used off-line to estimate combiner performance by estimating the SNR in each channel, which was done for data taken during a Jupiter track at DSS 13.

I. Introduction

The advantages of array feed combining for recovering signal-to-noise ratio (SNR) lost to mechanical deformations of large receiving antennas have been described in previous articles [1,2]. Typically, SNR losses become significant when carrier wavelengths smaller than the design tolerance of the reflector are employed. This is the case in the DSN, where Ka-band (33.7-GHz) reception is contemplated with the large 34- and 70-m antennas, whose surfaces are subject to considerable deformation from gravity and wind.

The array feed compensation system currently being evaluated at DSS 13 has been designed to recover SNR losses at both low and high elevations, where losses are most severe. The idea is to collect some of the deflected